WIRE-ROPE BRACING SYSTEM WITH ELASTO-PLASTIC DAMPERS FOR SEISMIC RESPONSE REDUCTION OF STEEL FRAMES

X. Hou[1] and H. Tagawa[2]

[1] *Graduate Student, Graduate School of Environment Studies, Nagoya University, Nagoya, Japan*
[2] *Associate Professor, Graduate School of Environment Studies, Nagoya University, Nagoya, Japan*
Email: tagawa@genv.nagoya-u.ac.jp

ABSTRACT:

Elasto-plastic dampers can reduce story drift of the frames and retain elasticity of structural members by adding hysteretic damping and stiffness. Extremely severe earthquakes, however, might cause large story displacement even for frames with the dampers. This paper presents a new bracing system for preventing large story displacement. The system uses wire ropes as brace members to eliminate brace-buckling entirely. The braced frames can increase the lateral strength without reducing energy dissipation characteristics of the moment frames by delaying the brace action. Comparison of the loading test results for the portal steel moment frames with and without wire-rope bracing members shows the fundamental characteristics of the bracing system. Numerical response analyses are performed for the three-story moment-resisting frames with and without the bracing and damping members. The characteristics and effectiveness of the bracing system are discussed in light of those test and analysis results.

KEYWORDS: bracing, elasto-plastic damper, loading test, seismic response analysis

1. INTRODUCTION

Damage to structures suffered in recent large earthquakes has emphasized the necessity of rehabilitating existing structures to withstand seismic events. Energy dissipation devices of several types have been investigated for the seismic upgrading of flexible steel frames (Bruneau and Bhagwagar 2002, Baratera and Giacchetti 2004, Xie 2005, Renzi et al. 2007). Elasto-plastic dampers in regions of high seismicity are commonly employed to retain elasticity of structural members during earthquakes. Large amount of plastic deformation capacity is expected in dampers to dissipate seismic energy. However, unexpected events, such as extremely severe earthquakes, might cause large story displacement, even for frames with dampers.

This study explores an application of the displacement-control-type bracing system (Tagawa and Hou 2007) for reducing the seismic response of steel frames with elasto-plastic dampers. The method uses wire-rope bracing to eliminate brace-buckling problems entirely. It controls the maximum story displacement. Application of the cable members to the hinge restrainer has been popular for seismic retrofitting of bridge structures. The displacement-control-type bracing system restrains lateral story displacement to within a specified range without reducing the energy dissipation capacity of the frames. The bracing members do not act for small and medium vibration amplitudes. For large vibration amplitudes, the bracing member acts and prevents unacceptably large story drift.

The effectiveness of the wire-rope bracing system for moment-resisting frames was demonstrated in previous studies by the authors through seismic response analyses and cyclic loading tests. The seismic response analysis results revealed that the bracing system has a re-centering effect on the vibration center and a deformation dispersion effect along the height. In those studies, the energy dissipation in the moment-resisting frames was considered. In addition to moment-resisting frames, this study uses hysteretic dampers as energy dissipation elements. In this paper, cyclic loading tests of portal moment frames demonstrate the fundamental characteristics of the proposed bracing system. Seismic response analyses conducted for three-story moment-resisting frames with and without the bracing and damping members reveal the effectiveness of the proposed bracing system.

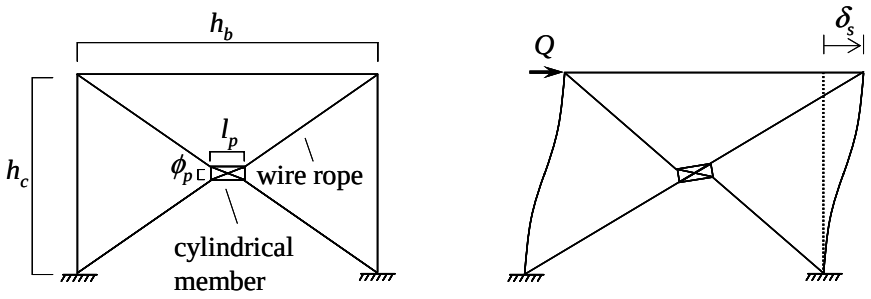

(a) Dimensions (b) Deformation at $\delta=\delta_s$

Figure 1 Displacement-restraint bracing system with wire ropes (Tagawa and Hou 2007)

2. OUTLINE OF DISPLACEMENT-RESTRAINT BRACING

The proposed bracing system concept is illustrated in Figure 1. The wire-rope bracing member is longer than the frame diagonal. A couple of wire-ropes are bundled with the cylindrical member of length l_p and inner diameter ϕ_p. In this system, the bracing members do not act between $\delta < \delta_s$, where δ equals the story drift and δ_s represents the story drift at which one bracing member becomes linear, as presented in Figure 1(b). Therefore, the behavior of the braced frame can keep energy dissipation characteristics similar to those of the moment-resisting frames for small and medium vibration amplitudes. In the large vibration amplitude, the bracing member acts and prevents unacceptably large story drift. Figure 1(b) shows that flexible wire-ropes, e.g. steel strand cables, must be used to exhibit the deformed configuration. The story drift δ_s is determined considering both the allowable story drift and the expected energy dissipation capacity of the frame. Plastic deformation of the wire-rope bracing members is not expected because of the members' low ductility. Consideration of a column axial force increment is necessary for avoiding catastrophic failure caused by bracing when this system is used for the seismic retrofit of existing frames.

The story drift δ_s at which the bracing member starts acting can be controlled according to the cylindrical member size, as shown in the following expression.

$$\delta_s = \sqrt{\left(2l_B + d_p\right)^2 - h_c^2} - h_b \tag{2.1}$$

where h_c and h_b respectively denote the column and beam length, and

$$d_p = \sqrt{l_p^2 + (\phi_p - \phi_B)^2}\ , \quad l_B = \sqrt{\left(\frac{h_b - l_p}{2}\right)^2 + \left(\frac{h_c - \phi_p}{2}\right)^2}\ , \tag{2.2), (2.3}$$

where l_p and ϕ_p respectively denote the length and inner diameter of the cylindrical member. Also, ϕ_B signifies the wire rope diameter.

3 LOADING TESTS

3.1. Test specimens

Figure 2 presents the test specimens. The column and beam members of H-150×150×7×10 were connected with bolted T-stubs cut from H-300×150×6.5×9. Only the T-stubs exhibited plastic deformation during the tests: the column and beam members remained elastic. The bracing members of the wire rope were 12-mm-diameter stainless steel (SUS 316) strand (7×19) cables. Turnbuckles were used to pull in the slack of the wire ropes. The following three specimens were tested.

Specimen A: Moment-resisting frame without bracing.
Specimen 12B: Moment-resisting frame with the proposed bracing system.
Specimen 12C: Moment-resisting frame with typical bracing.

The cylindrical member used in specimen 12B was made of chlorinated polyvinyl chloride; the member sizes were l_p = 266 mm and ϕ_p = 51 mm. For this case, δ_s = 40 mm was obtained from Eqn. (2.1).

3.2. Test setup and procedure

Figure 3 depicts the test setup. The columns were supported by pin supports at the bottom. The test frames were loaded cyclically by a 1000 kN capacity hydraulic jack with a 300 mm stroke. Out-of-plane movement of the frames was prevented at the column tops, as depicted in Photo 1. Figure 4 shows the applied loading history under displacement control using the story drift, δ, measured during the test.

3.3. Test results

Figure 5 shows the lateral load and the lateral displacement relationships of the specimens. For specimens A and 12B, local buckling of the T-stub web occurred at the final stage. For specimen 12C, the bracing member was broken at point J. The skeleton curves are portrayed in Figure 6, where the broken lines give the initial stiffness. Table 1 shows the initial stiffness k, maximum load P_{max}, and ultimate displacement δ_u for each specimen. Furthermore, the ratios of each value with respect to specimen A are shown. The ultimate displacement for specimens 12C represents the value at point J.

The bracing member did not act until δ_s = 40 mm for specimen 12B. For that reason, the initial stiffnesses k of specimens A and 12B are almost identical. In contrast, the initial stiffness of specimen 12C is about 1.55 times that of specimen 12B. The maximum load P_{max} for specimen 12B is the largest among the specimens; also, the difference between 12B and 12C is small. By contrast, for the ultimate displacement δ_u, the difference between 12B and 12C is large. The value of δ_u for 12B is about 1.12 times that of specimen A, while that of 12C is only 0.66 times that of specimen A. These results demonstrate the large deformation capacity of the proposed bracing system. Photo 1 shows the deformed configuration of specimen 12B at δ = 40 mm.

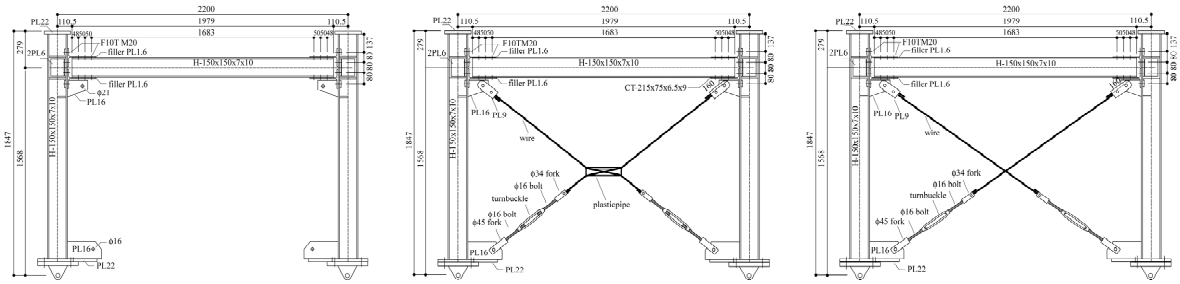

(a) Specimen A (b) Specimen 12B (c) Specimen 12C

Figure 2 Test specimens

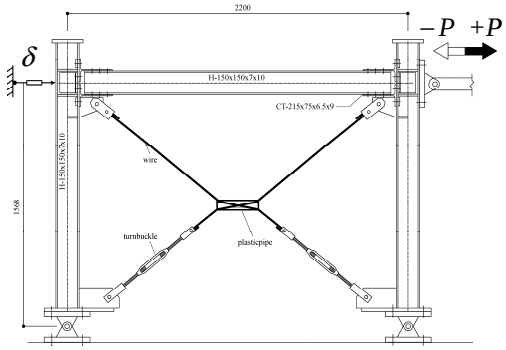

Figure 3 Test setup

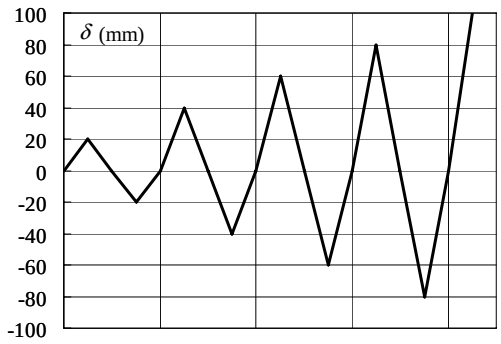

Figure 4 Loading history

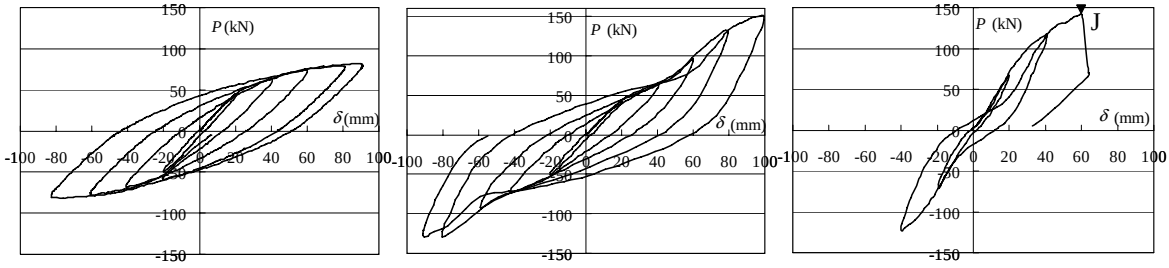

(a) Specimen A (b) Specimen 12B (c) Specimen 12C

Figure 5 Load and displacement relationships

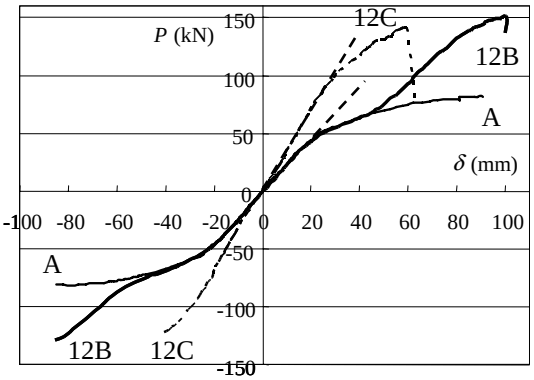

Figure 6 Skeleton curves

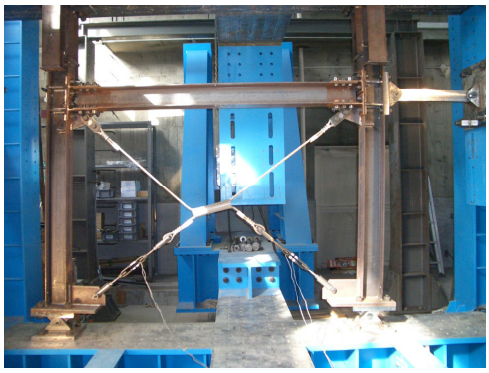

Photo 1 Deformed configuration (12B)

Table 1 Test results

Specimen	k (kN/mm)	k/k_A	P_{max} (kN)	P_{max}/P^A_{max}	δ_u (mm)	δ_u/δ^A_u
A	2.24	1	82	1	90	1
12B	2.3	1.03	151	1.84	100	1.12
12C	3.59	1.6	142	1.73	60	0.66

4 SEISMIC RESPONSE ANALYSIS

4.1. Analysis Model

4.1.1 Model description

For examining the effectiveness of the proposed bracing system, seismic response analyses were performed for the three-story frames. Figure 7 shows the analysis models composed of the bare frame (Model F), the frame with dampers (Model D), and the braced frame with dampers (Model DB). The shear-type frame models were used to highlight the improvement of the frame behavior by bracing. Only the column and damper members exhibited elastic-plastic behavior with a strain hardening ratio of 0.001; the beam members were assumed to be rigid; the bracing members were assumed to remain elastic. The members were considered to have the same cross-section from the first to third story. The structural properties were first determined for the bare frame. The square hollow structural section of 200 mm depth and width and 8 mm thickness was selected for the column members considering the condition that the story drift angle for each story was smaller than 0.005 rad against the design earthquake force profile with the base shear coefficient (ratio of shear force at the first story to the total frame weight) of 0.2. The lateral strength of the bare frame was obtained by ultimate analysis as the base shear coefficient of 0.52 considering the yield stress of 300 MPa for the column members.

4.1.2 Damper property

Figure 8 illustrates the story shear and story drift relationships. For the bare frame, the yield story shear, the yield story drift, and the initial stiffness are denoted respectively by Q_{fy}, δ_{fy}, and K. For the damping device, a

shear-panel-type elasto-plastic damper was selected. Note that the damper contribution was considered only for the story shear and story drift relationships. The damper stiffness is about twice that of the bare frame, and the damper ultimate strength is about 0.5 times that of the bare frame. The damper exhibits bi-linear type elasto-plastic behavior with a strain hardening ratio of 0.001.

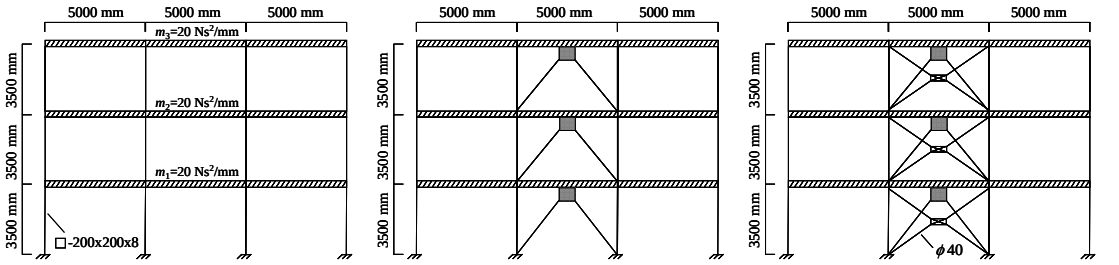

(a) Bare frame (Model F) (b) Frame with dampers (Model D) (c) Braced frame with dampers (Model DB)

Figure 7 Model frames

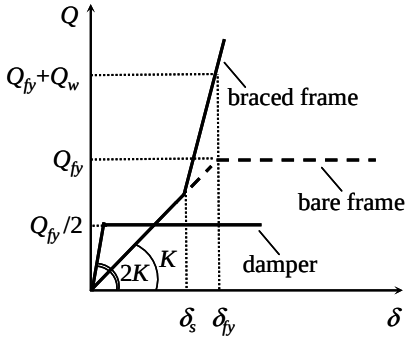

Figure 8 Story shear and drift relationships

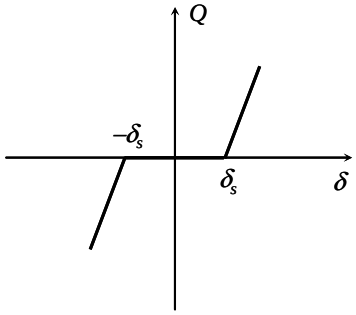

Figure 9 Q–δ relationships of bracing

4.1.3 Braced frame with dampers

The concept of determining the properties of bracing members is illustrated in Figure 8. To reduce the plastic deformation in the moment frame, the value of δ_s is determined in a manner that the story shear of the braced frame reaches $Q_{fy}+Q_w$ at $\delta=\delta_{fy}$, where Q_w = the increment of the story shear strength using wire-rope bracing. The value of Q_w is obtained from

$$Q_w = \frac{P_{wu} h_b}{\nu \sqrt{h_b^2 + h_c^2}}, \tag{4.1}$$

where P_{wu} represents the ultimate strength of the wire rope and ν is the control parameter. For determining the dimension of bracing members, some preliminary seismic response analyses were conducted without dampers; the values of $Q_w = 0.7Q_{fy}$ and $\nu = 4$ were chosen using the strand wire rope with 40 mm outer diameter. For the case of ground motions shown in Table 2, the maximum axial force of the wire-rope was about 0.83 P_{wu} and the maximum increment of axial force ratio of the columns was about 0.17, which indicates that the axial force of the members was maintained within the allowable range. A simulation software package (SNAP Ver.4, 2007) was used throughout this study. Instead of considering geometrical nonlinearity for representing the brace behavior, multi-linear relationships were considered for brace elements in a manner that Q-δ curves attributable to bracing exhibited a relationship like that shown in Figure 9.

4.2. Seismic Response Analysis Results

Four earthquake records were used for input ground motions. Each acceleration record was scaled so that the maximum velocity was equal to 50 cm/s and 70 cm/s, as presented in Table 2. The seismic duration of 20 s was considered for all motions. The average acceleration method was applied for the numerical integration of equations of motion. Stiffness proportional damping was considered with a 2% damping ratio for the first mode. Eigenvalue analysis yielded the fundamental natural period of the bare frame (Model F) and the frame with dampers (Model D) as 0.69 s and 0.40 s, respectively.

4.2.1 Maximum story drift angle

Figure 10 depicts a comparison of the maximum story drift angle distributions. As described previously, the shear-type analysis models have the same cross section of columns from the first to third story. This induces the largest story rotation in the first story of the bare frame (Model F). For ground motions of maximum velocity 50 cm/s, the story drift distribution of the frame with dampers (Model D) is almost the same as that of the braced frame with dampers (Model DB), which indicates that the bracing system worked slightly for those cases. In contrast, for 70 cm/s ground motions, model D exhibits a large drift angle in the first story, whereas the drift angle for the model DB is restrained within about 0.01 rad. It is noteworthy that, for the Taft and JMA-Kobe motions, the story drift in the second and third story of Model DB is greater than that of Model D, which demonstrates that the proposed bracing system has a deformation dispersion effect along the height and prevents seismic energy concentration into the local story.

Table 2 Seismic ground motions used in the analysis

Input motion	Max. V.	Max. Acc.	Duration
El Centro 1940 NS	50 cm/s	510.8 cm/s^2	20 s
	70 cm/s	715.1 cm/s^2	
Taft 1952 EW	50 cm/s	496.9 cm/s^2	20 s
	70 cm/s	695.7 cm/s^2	
Hachinohe 1968 NS	50 cm/s	329.9 cm/s^2	20 s
	70 cm/s	461.9 cm/s^2	
JMA-Kobe 1995 NS	50 cm/s	449.9 cm/s^2	20 s
	70 cm/s	629.9 cm/s^2	

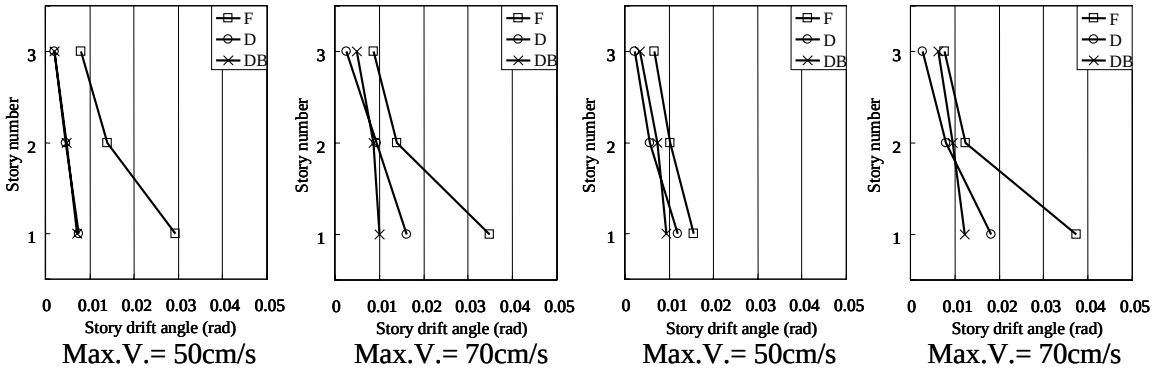

Max.V.= 50cm/s Max.V.= 70cm/s Max.V.= 50cm/s Max.V.= 70cm/s

(a) El Centro NS (b) Taft EW

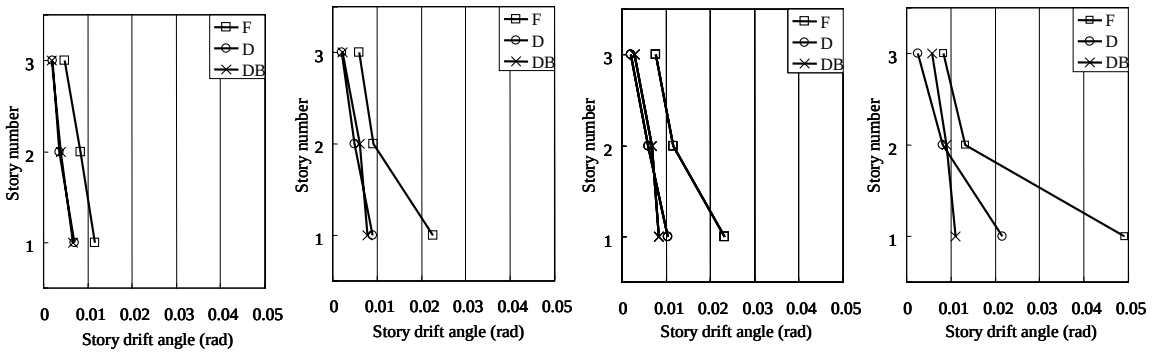

Max.V.= 50cm/s Max.V.= 70cm/s Max.V.= 50cm/s Max.V.= 70cm/s

(c) Hachinohe NS (d) JMA-Kobe NS

Figure 10 Comparison of the story drift angle distribution

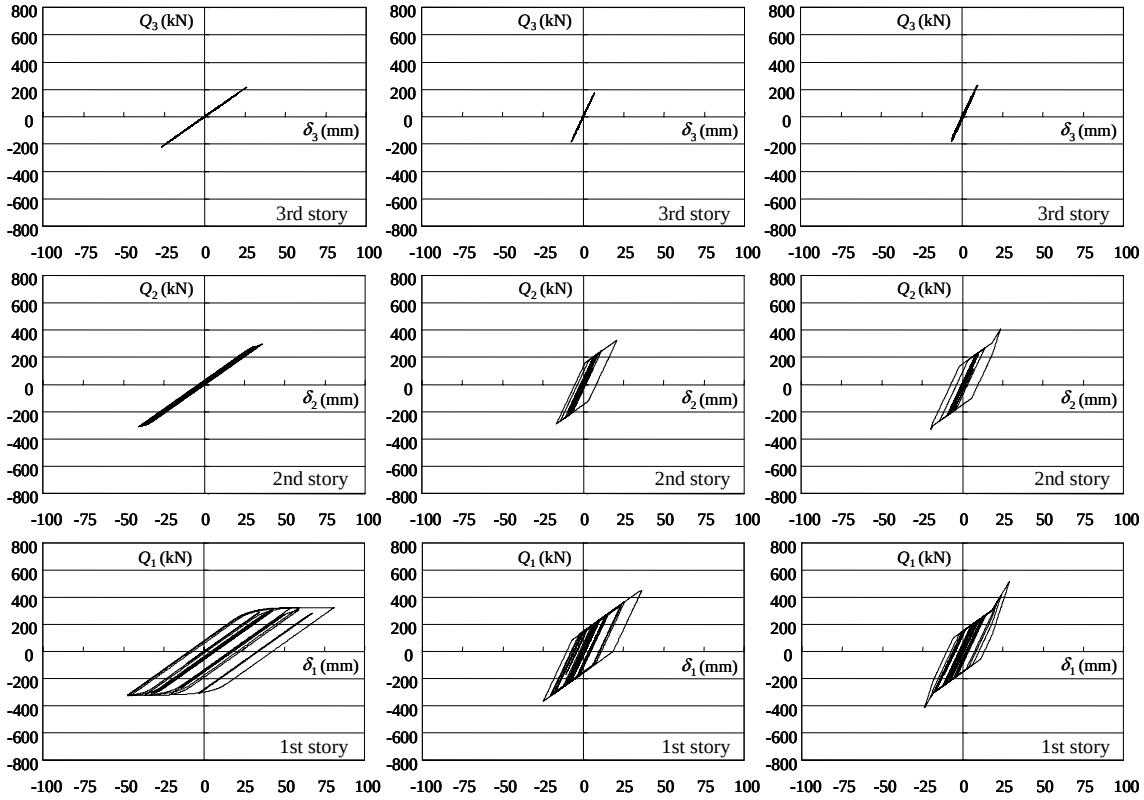

(a) Model F (b) Model D (c) Model DB

Figure 11 Story shear – story drift relations for JMA-Kobe NS (Max. V.=50 cm/s)

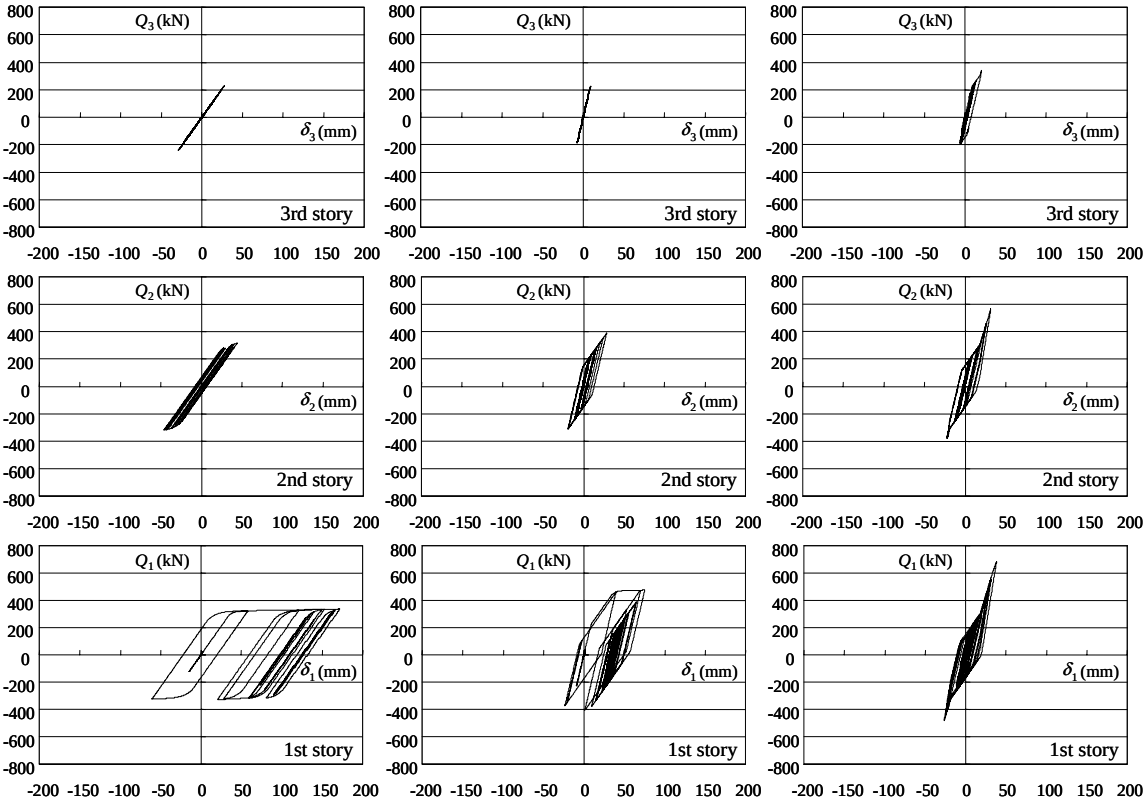

(a) Model F (b) Model D (c) Model DB

Figure 12 Story shear – story drift relations for JMA-Kobe NS (Max. V.=70 cm/s)

4.2.2 Story shear and story drift relationships

Story shear and story drift relationships for the JMA-Kobe motion are selected to demonstrate the effectiveness of the proposed bracing system. Figures 11 and 12 respectively depict the results obtained for the cases of 50 cm/s and 70 cm/s maximum velocity. The first story of Model F exhibits the largest story drift, especially for the case of 70 cm/s, where a large residual deformation is also observed. For Model D, hysteretic dampers dissipate seismic energy. For that reason, the frame members remained within the elastic range for the case of 50 cm/s. For 70 cm/s, however, the frame members exhibit plastic deformation; consequently, residual deformation is observed for Model D. Although the maximum story shear is rather large for Model DB for 70 cm/s, the residual deformation in the first story was reduced dramatically, which demonstrates that the proposed retrofit method has a strong effect for re-centering the vibration center.

5. CONCLUSIONS

This study investigated application of a displacement-restraint bracing to steel moment frames with elasto-plastic dampers. The bracing system comprises two wire ropes and a cylindrical member that bundles wire ropes. Cyclic loading tests of the portal moment frames demonstrated the fundamental characteristics of the proposed bracing system. The braced frames can increase the lateral strength without reducing energy dissipation characteristics of the moment frames by delaying the brace action.

Seismic response analyses were conducted for three-story frame models with elasto-plastic dampers. The results revealed that the proposed bracing system can restrain story drift to within the specified range under severe seismic motions. The bracing system has a re-centering effect on the vibration center and a deformation dispersion effect along the height.

REFERENCES

Bruneau, M. and Bhagwagar, T. (2002). Seismic retrofit of flexible steel frames using infill panels. *Engineering Structures* **24**, 443-453.

Bartera, F. and Giacchetti, R. (2004). Steel dissipating braces for upgrading existing building frames. *Journal of Constructional Steel Research* **60**, 751-769.

Renzi, E., Perno, S., Pantanella, S., and Ciampi, V. (2007). Design, test and analysis of a light-weight dissipative bracing system for seismic protection of structures. *Earthquake Eng. Struct. Dyn.* **36**, 519-539.

SNAP Ver.4. (2007). Kozo System, Inc. Tokyo, JAPAN.

Tagawa, H. and Hou, X. (2007). Seismic retrofit of ductile moment resisting frames using wire-rope bracing. *Proceedings of the Eighth Pacific Conference on Earthquake Engineering*, Singapore.

Xie, Q. (2005). State of the art of buckling-restrained braces in Asia. *Journal of Constructional Steel Research* **61**, 727-748.